Maximum leaf conductance driven by CO_2 effects on stomatal size and density over geologic time

Peter J. Franks[1] and David J. Beerling

Department of Animal and Plant Sciences, University of Sheffield, Sheffield S10 2TN, United Kingdom

Communicated by Robert A. Berner, Yale University, New Haven, CT, April 20, 2009 (received for review February 3, 2009)

Stomatal pores are microscopic structures on the epidermis of leaves formed by 2 specialized guard cells that control the exchange of water vapor and CO_2 between plants and the atmosphere. Stomatal size (*S*) and density (*D*) determine maximum leaf diffusive (stomatal) conductance of CO_2 ($g_{c_{max}}$) to sites of assimilation. Although large variations in *D* observed in the fossil record have been correlated with atmospheric CO_2, the crucial significance of similarly large variations in *S* has been overlooked. Here, we use physical diffusion theory to explain why large changes in *S* necessarily accompanied the changes in *D* and atmospheric CO_2 over the last 400 million years. In particular, we show that high densities of small stomata are the only way to attain the highest g_{cmax} values required to counter CO_2''starvation'' at low atmospheric CO_2 concentrations. This explains cycles of increasing *D* and decreasing *S* evident in the fossil history of stomata under the CO_2 impoverished atmospheres of the Permo-Carboniferous and Cenozoic glaciations. The pattern was reversed under rising atmospheric CO_2 regimes. Selection for small *S* was crucial for attaining high g_{cmax} under falling atmospheric CO_2 and, therefore, may represent a mechanism linking CO_2 and the increasing gas-exchange capacity of land plants over geologic time.

Phanerozoic | photosynthesis | plant evolution | transpiration | xylem

Stomata crucially permit plants to regulate transpirational water loss from leaves during the simultaneous uptake of CO_2 for photosynthesis (1, 2). Originating more than 400 Ma, their evolutionary appearance was pivotal to the colonization of the land by plants, permitting the survival and ecological radiation of floras throughout diverse terrestrial habitats experiencing widely fluctuating environmental conditions (2–4). Remarkably, the fundamental design of stomata has remained unchanged over the 400-million year (Myr) history of vascular plants (3, 4) but has been fine-tuned through increases in the operational efficiency of guard cell function (5). Nevertheless, major changes in stomatal size (*S*) and density (*D*) are evident in the fossil record (2, 6) (Fig. 1; Table S1), but their significance as land-plant evolution progressed, in parallel with advancements in gas-exchange capacity, is not yet understood. Here, we use diffusion theory and Earth's global atmospheric CO_2 history to provide a unifying functional explanation for these changes in stomatal geometry over evolutionary time scales.

One basic feature of leaves that should be highly conserved is the relationship between maximum pore area and leaf gas-exchange capacity, which is governed by the physics of diffusion through pores. The maximum area of the open stomatal pore (a_{max}) and its depth (l) are set by stomatal size *S* (defined here as guard cell length, *L*, multiplied by total width, *W*, of the closed guard cell pair). Taken together, a_{max}, l, and *D* determine maximum diffusive conductance to water vapor or CO_2 (g_{wmax} or g_{cmax}, respectively) according to ref. 7:

$$g_{wmax} = \frac{d}{v} \cdot D \cdot a_{max} \Big/ \left(l + \frac{\pi}{2} \sqrt{a_{max}/\pi} \right), \qquad [1]$$

where d is the diffusivity of water vapor in air ($m^2 \cdot s^{-1}$), v is the molar volume of air ($m^3 \cdot mol^{-1}$), and $g_{cmax} = g_{wmax}/1.6$ (1).

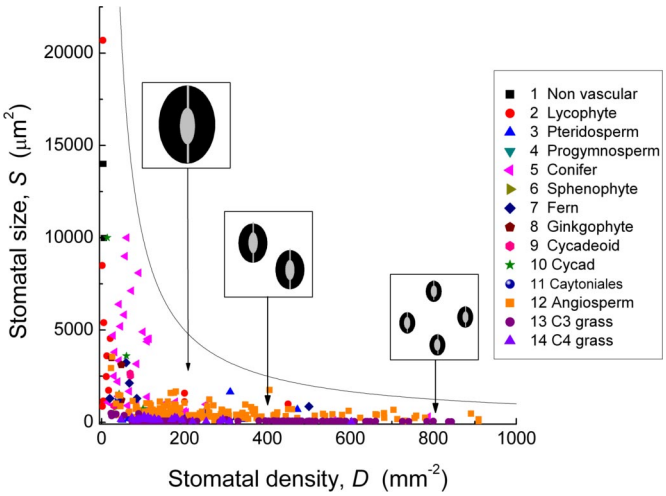

Fig. 1. The relationship between stomatal size *S* and density *D* across the Phanerozoic. Each point is an individual species (see Table S1). The curved line is the estimated upper theoretical limit to stomatal size at a given density, or the upper limit of density at a given size. All combinations of size and density must fall below this line. Diagrams in boxes are comparative representations of possible combinations of stomatal size and density to assist visualization of the scaling of these dimensions in real leaves.

Critically, it can be shown mathematically that for the same total pore area, a_{max}, smaller stomata result in higher g_{wmax} compared with larger stomata (Fig. 2). This is because g_{wmax} is inversely proportional to the distance that gas molecules have to diffuse through the stomatal pore (l), which increases with *S* as guard cells inflate to be approximately circular in cross-section (5). It can be further shown, by using Eq. **1**, that for a given g_{wmax}, smaller stomata allow more epidermal space to be allocated to other structures such as subsidiary cells, trichomes, or oil cells (Fig. 3). Stomatal size is important not only to g_{wmax} and g_{cmax} but also to the overall structure and broader ecophysiological function of leaf surfaces.

The 400-Myr fossil history of stomata reveals that although *S* and *D* have both varied by several orders of magnitude (Fig. 1), all reported combinations are located within the biophysical envelope defined by maximum packing of stomata on the leaf surface (i.e., the maximum number of stomata of a given size, *S*, that can fit within a unit area) (Fig. 1; Table S1). Indeed, combinations of *S* and *D* must lie somewhat below this upper packing limit to accommodate several developmental, physiological, and mechanical requirements for spacing of stomata (5, 8).

Author contributions: P.J.F. and D.J.B. designed research, performed research, analyzed data, and wrote the paper.

The authors declare no conflict of interest.

Freely available online through the PNAS open access option.

[1]To whom correspondence should be addressed. E-mail: p.franks@sheffield.ac.uk.

This article contains supporting information online at www.pnas.org/cgi/content/full/0904209106/DCSupplemental.

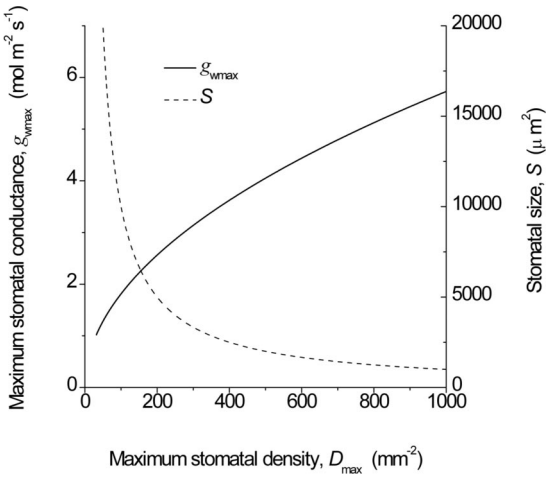

Fig. 2. Smaller stomata provide higher stomatal conductance for the same total pore area because of the shorter diffusion path length, *l* (see Eq. **1**). For any stomatal size *S* there is a theoretical maximum stomatal density D_{max} based on simple geometric packing limitations. Here the total stomatal pore area per unit leaf area remains constant at the theoretical maximum for any given stomatal size *S*, but because that pore area is made up of ever-smaller and more numerous stomata, the stomatal conductance (g_{wmax}) increases. See *Data and Methods* for details.

Irrespective of the size, shape, or number of epidermal cells filling the space between individual stomata on a leaf surface, *S* and *D* are virtually the only epidermal characteristics determining g_{cmax}, an important feature constraining maximum leaf gas-exchange capacity. At the time of first appearance of vascular plants in the fossil record, atmospheric CO_2 concentration was several times higher than current ambient CO_2 (9), but subsequent periods of falling atmospheric CO_2 challenged plants with diminished CO_2 availability. Adaptation of g_{cmax} to these conditions required a change in *S* and/or *D*, and we hypothesize from principles of stomatal packing on leaf surfaces (Figs. 2 and 3) and gas-exchange diffusion theory (Eq. **1**) that selection for higher g_{cmax} by falling atmospheric CO_2 is characterized by a trend toward smaller *S* and higher *D*.

Results

Consistent with our hypothesis we report that a positive correlation between *S* and Earth's global atmospheric CO_2 history

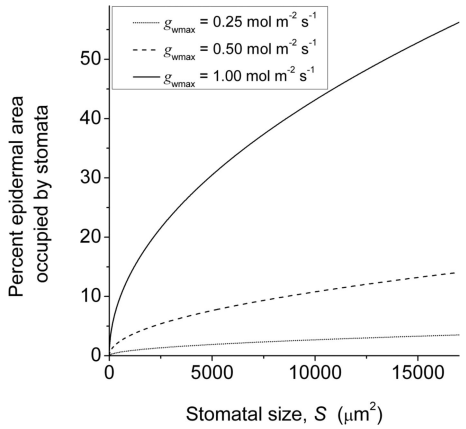

Fig. 3. For any given g_{wmax}, smaller stomata free up more epidermal space for other cell types and functions. Shown are percentages of epidermal surface occupied by stomata as a function of variable stomatal size *S* for 3 fixed values of g_{wmax}. CO_2-forcing of changes in g_{wmax} via changes in *S* and *D* have implications for leaf attributes unrelated to g_{wmax}. See *Data and Methods* for details.

(Fig. 4*A*) is mirrored by a negative correlation between *D* and CO_2 over hundreds of millions of years of plant evolution (Fig. 4*B*). The magnitude of change in *S* is far greater than, but consistent with, that observed in short-term CO_2 experiments (Table 1). These short-term changes are presumably reflecting phenotypic plasticity (i.e., the limited range in magnitude of *S* resulting from the effect of changes in the environment on stomatal development within a single generation). The strong negative correlation of *D* with CO_2 over 400 Myr (Fig. 4*B*) is consistent with observations on Quaternary fossil leaves over documented glacial–interglacial CO_2 changes (10, 11), trees experiencing the rapid rise in atmospheric CO_2 over the past century (12), and experiments (13).

The functional consequence of the tradeoff between *S* and *D* allows g_{wmax} and g_{cmax} to increase as global atmospheric CO_2 declines (Fig. 4*C*). The requirement for large numbers of small stomata to maximize gaseous CO_2 diffusion into leaves for higher rates of photosynthesis (Fig. 2) is indicated by the negative correlation between g_{wmax} and *S* (Fig. 4*D*). Large numbers of small stomata, linked to a decrease in atmospheric CO_2, could potentially also allow transpiration rates to rise. However, on the multi-million year time scale involved, the climate would also be expected to cool through a weakening of the atmospheric greenhouse effect and thereby diminish the driving force for evaporation from leaves.

The inability of large stomata to sustain high g_{wmax} is illustrated in Fig. 5. Color contours representing constant g_{wmax} for various combinations of *S* and *D* show that as *S* decreases, higher values of g_{wmax} become possible, as delineated by the increasing range of colors falling below the theoretical maximum (black line). Throughout the entire 400-Myr history of land-plant evolution, 2 distinct modes of change in stomatal *S* and *D* occur repeatedly in the fossil history of stomata, as revealed by *S* versus *D* cross-plots for five 50- or 100-Myr intervals (symbols in Fig. 5). Coordinated changes in *S* and *D* occur against a consistent pattern of CO_2 change or regime, as estimated by geochemical carbon cycle modeling (9) that is validated against independent proxy estimates (14).

The first mode emerges for plants experiencing a relatively stable, high-CO_2 atmosphere with nonglacial climates and is characterized by low densities of stomata (*D*), but with 10-fold variations in size (*S*) (Fig. 5 *A*, *C*, and *D*). These combinations of *S* and *D*, characterized by predominantly large *S* and small *D*, restrict g_{wmax} to low values. The pattern is consistent across a wide range of evolutionary life histories, from homosporous early vascular plants, such as *Cooksonia* in the CO_2-rich atmosphere of the Silurian (Fig. 5*A*), through to advanced gymnosperm and angiosperm trees experiencing "greenhouse" conditions in the Jurassic and Cretaceous (Fig. 5*D*). Similar responses of *S* and *D* are observed in modern plants under drought treatment, whereby *S* often becomes smaller, with minor increases in *D* (15–17). Conditions of simulated water stress via treatment with abscisic acid, a plant hormone released under water stress, induce a similar response (7). Ultimately in these circumstances, reductions in *S* tend to be proportionally greater than any increases in *D*, reducing g_{wmax} and improving the water-use economies of leaves (7, 17).

The second distinct mode of change in stomatal traits emerges when atmospheric CO_2 is falling and the Earth system is transitioning from a predominant "greenhouse" to "icehouse" state (Fig. 5 *B*, *E*, and *F*). Falling atmospheric CO_2 levels during glacial inceptions are accompanied by large variations in fossil density (*D*), but generally small stomates (*S*), allowing plants to operate with a higher g_{wmax}. This pattern occurs repeatedly as CO_2 levels drop during the onset of the Permo-Carboniferous glaciation (Fig. 5*B*), the long-term cooling leading to the Cenozoic glaciation (Fig. 5*E*), and the current icehouse world characterized by a geological interval

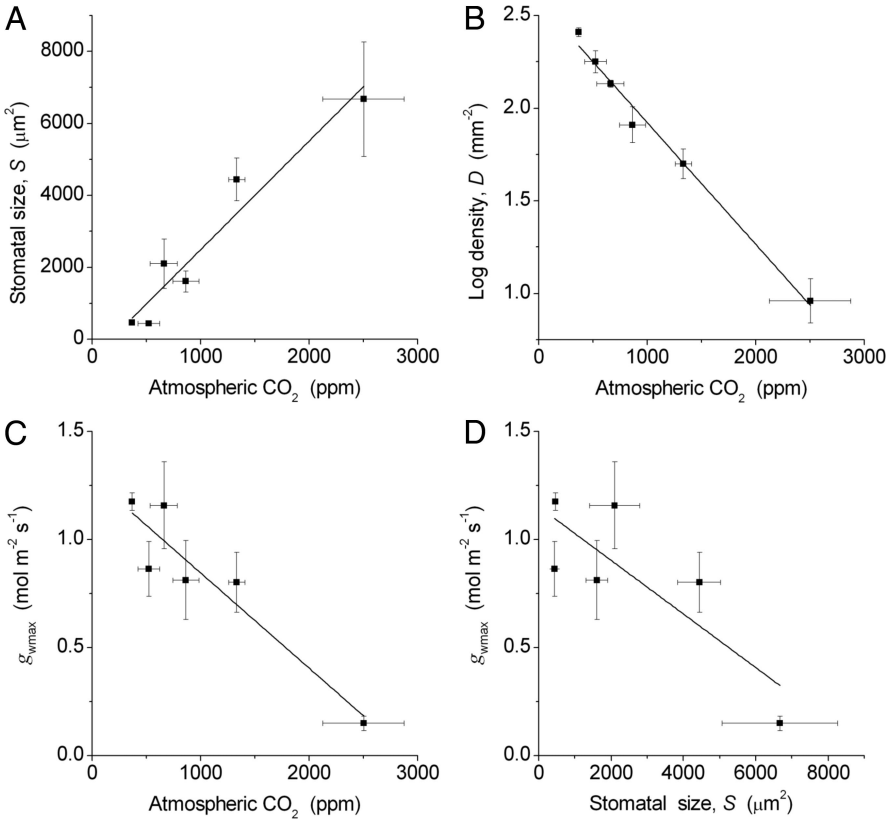

Fig. 4. Relationships between fossil stomatal traits and atmospheric CO_2. Each point is the mean for either a 50- or 100-Myr time slice of the Phanerozoic, beginning at −400 Myr, or the mean for modern times (0 Myr). (*A*) Stomatal size is positively correlated with atmospheric CO_2 concentration ($y = 3.02x - 528$; $r^2 = 0.92$; $P < 0.002$). (*B*) Stomatal density *D* decreases exponentially with atmospheric CO_2 concentration, hence $\log_{10}D$ is linearly correlated with CO_2 ($y = -0.000657x + 2.58$; $r^2 = 0.98$; $P < 0.0001$). (*C*) Maximum stomatal conductance to water vapor, g_{wmax}, is negatively correlated with atmospheric CO_2 concentration ($y = -0.000441x + 1.29$; $r^2 = 0.84$; $P < 0.006$). (*D*) g_{wmax} is negatively correlated with stomatal size *S* ($y = -0.000124x + 1.15$; $r^2 = 0.60$; $P = 0.04$).

of low CO_2 (Fig. 5*F*). It mirrors the effects of changes in atmospheric CO_2 on the stomata of extant plants (12, 13, 17, 18) and holds even for grasses evolving in the low-CO_2 atmosphere of the Miocene.

High g_{wmax} values contribute significantly to alleviating the negative impact of diminishing CO_2 availability on photosynthesis at these times by increasing CO_2 diffusion into leaves and can only be attained with considerable reduction in *S* in combination with high *D*. Having fewer, larger stomata cannot achieve the same effect because of concomitant increases in the length of the diffusion pathway through the pore (Fig. 2). A possible additional advantage to having flexibility in *D* relates to energetic cost. The energetic requirements of running stomata are proportionally small in relation to the respiratory costs of the whole leaf (19) but locally, as a fraction of epidermal tissue costs, may be significant. The guard cell respiratory cost in high-conductance cotton varieties, for example, is about twice that of low-conductance varieties (20). The flexibility to reduce *D* when environmental conditions demand lower g_{wmax} might, therefore, also constitute a metabolic cost-saving mechanism.

Discussion

Our analyses implicate long-term global atmospheric CO_2 change as a continuous driver of increasing g_{wmax} and g_{cmax} throughout the entire evolutionary history of vascular plants (Fig. 4*C*). The analyses identify a previously unrealized effect of CO_2 on stomatal size that is consistent with the direction of change observed in plant CO_2-enrichment experiments for a grass, C_4 herb, and an angiosperm C_3 tree (Table 1). Our study

Table 1. Increase in stomatal size, *S*, in response to growth at elevated atmospheric CO_2 (short-term experiments)

Species	*S* at low CO_2, μm^2	*S* at high CO_2, μm^2	*S* increase, %	Ref.
Zea mays	918	1,072	16.78	18
Oryza sativa cv. Pusa Basmati-1	209	231	10.53	31
O. sativa cv. P-677	155	281	81.29	31
O. sativa cv. P-834	185	251	35.68	31
O. sativa cv. P-2503-6-693	160	222	38.75	31
Betula pubescens	618	705	14.08	32

Low CO_2 treatment: 350 ppm; high CO_2 treatment: 700 ppm.

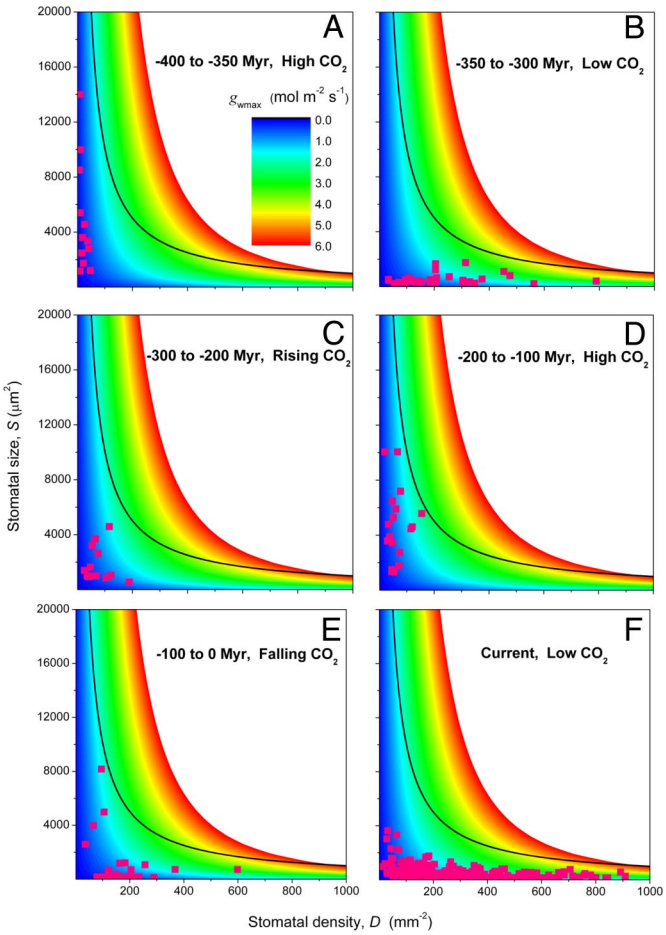

Fig. 5. Distinct modes of stomatal trait evolution. Graduations in g_{wmax} for multiple combinations of S and D are represented by color contours. The curved black line represents the theoretical upper limit of S versus D. Note that g_{wmax} at this limit increases with D, even though S decreases. Stomatal conductances attainable at small S and high D are theoretically unattainable at much larger S and lower D (red area), even though total pore area per unit leaf area is constant. Overlaid on this surface are data (pink symbols) for S and D from fossil plants, showing the predominance of smaller S and higher D in times of falling atmospheric CO_2 concentration.

highlights the functional interdependence of S and D, particularly the inability of large S to support high g_{cmax}, while reinforcing the more widely recognized effect of CO_2 on D (12, 21, 22). We are not suggesting that atmospheric CO_2 has been the only driver on evolutionary time scales; other features of the climatic and ecological environment are also likely to be involved (2). However, the tight correspondence between changes in S and D with CO_2 is consistent with the biophysical requirements for increasing g_{cmax} under decreasing atmospheric CO_2 concentration and with physiological (23) and molecular (24) mechanisms linking plasticity of S and D with sensitivity to CO_2. If changing atmospheric CO_2 forced S to change by several orders of magnitude, then this mechanism has profound implications for the evolution of plant function in relation to cell size-dependent plant attributes.

The major physiological significance of the correlation of guard cell size, stomatal density, and g_{cmax} with atmospheric CO_2 over millions of years suggests a mechanism connecting long-term CO_2 change with the ecological radiation of land plants. Reconstructions of g_{wmax} from S and D in the fossil record have shown a systematic increase over geologic time (25), a pattern that mirrors the rise in land-plant diversity (26) and the coevolution of vascular water-conducting capacity (27). The mechanistic linkage underpinning the similarity of these records remains to be understood, but with regard to stomatal size, there are additional dynamic properties inherent in small S that, coupled with the higher photosynthetic capacity accompanying high g_{wmax}, would enhance plant fitness in a broader range of environments. Smaller stomata are capable of faster response times (2, 5), enabling improved water-use efficiency and optimization of long-term carbon gain with respect to water loss (28). Stomata of most plants reduce their apertures to counteract potentially high transpiration rates in dry air or high wind speeds (29). Smaller, faster stomata would, therefore, minimize exposure to excessive water-potential gradients through the plant and help protect plants from xylem embolisms. Taken together, these ecophysiological traits permitted plants to occupy broader ecological and environment niches and allowed diversity to increase.

We conclude that the coevolution of plants' gas-exchange capacity and the geochemical carbon cycle has, therefore, likely been a continuous feature of the Earth system for 400 Myr, entraining a suite of planetary-wide feedbacks (30) arising through the action of CO_2 at the cellular scale of stomata. A better understanding of the processes involved will contribute to elucidating a mechanistic explanation for the rise in land-plant biodiversity over this geologic time period, as documented in the fossil record a quarter of a century ago (26).

Data and Methods

Stomatal Dimensions. All measures of S and D were obtained from published articles, acknowledging potential sampling bias and incompleteness of the paleobotanical literature. Data and sources are given in Table S1. Values were taken either directly as reported in the text or tables or, in some cases, measured from photomicrographs. Stomatal size S was calculated as guard cell length L multiplied by the width W of the guard cell pair. When W was not available, it was estimated as $L/2$ for nongrasses or $L/8$ for grasses. The theoretical maximum stomatal density D_{max} (in units of mm^{-2}) for any given stomatal size, indicated by the hyperbolic black line in Figs. 1, 2, and 5, was calculated as $1/S$, with S in units of mm^2 (i.e., D_{max} is 1 mm^2 divided by the area, in mm^2, of 1 stoma).

Calculating g_{wmax}. Maximum stomatal conductance to water vapor, g_{wmax}, was calculated by using Eq. **1**, with a_{max} approximated as $\pi(p/2)^2$, where p is stomatal pore length (Figs. 2, 4, and 5). When p was not available it was approximated as $L/2$ on the basis of information provided in ref. 5. Stomatal pore depth l for fully open stomata was taken as equal to guard cell width (i.e., $W/2$), assuming guard cells inflate to a circular cross-section. Values for standard gas constants d and v were those for 25°C. In Fig. 5, using S and D as inputs and p as $L/2$ (5), a matrix of g_{wmax} was generated and plotted as a graduated-color contour map (Fig. 5). Plots of S versus D for individual species in respective geological time periods were overlaid on this surface.

Calculating S for Fixed g_{wmax} and Variable D. (Fig. 3.) With respect to Eq. **1**, a_{max} was taken as $0.12S$, with 0.12 being midway between the range of pore-area/stoma-area ratios for fully open stomata reported in ref. 5. Rearranging Eq. **1** then gives $L \approx 6(g_{wmax} \cdot v)/(d \cdot D)$, from which S was approximated as $S = (L^2)/2$.

Statistical Analysis. The significance of correlations was tested by using linear regression, with P values of <0.05 considered statistically significant. Means were compared by using one-way analysis of variance and post hoc means comparison (Scheffé Test). All data analysis and plotting were performed with OriginPro 8.0 data analysis software (OriginLab Corporation, Northampton, MA).

ACKNOWLEDGMENTS. We thank Joe Berry, Mark Chase, Ian Cowan, Jeremy Beaulieu, Alistair Hetherington, Robert Berner, Ian Woodward, and Graham Farquhar for comments and discussion on this work. D.J.B. gratefully acknowledges receipt of an Edward P. Bass Environmental Scholarship at the Yale Institute of Biospheric Studies, Yale University.

1. Farquhar GD, Sharkey TD (1982) Stomatal conductance and photosynthesis. *Annu Rev Plant Physiol* 33:17–45.
2. Hetherington AM, Woodward FI (2003) The role of stomata in sensing and driving environmental change. *Nature* 424:901–908.
3. Edwards D, Kerp H, Hass H (1998) Stomata in early land plants: an anatomical and ecophysiological approach. *J Exp Bot* 49:255–278.
4. Raven JA (2002) Selection pressures on stomatal evolution. *New Phytol* 153:371–386.
5. Franks PJ, Farquhar GD (2007) The mechanical diversity of stomata and its significance in gas exchange control. *Plant Physiol* 143:78–87.
6. Beerling DJ, Woodward FI (1997) Changes in land plant function over the Phanerozoic: reconstructions based on the fossil record. *Bot J Linn Soc* 124:137–153.
7. Franks PJ, Farquhar GD (2001) The effect of exogenous abscisic acid on stomatal development, stomatal mechanics, and leaf gas exchange in *Tradescantia virginiana*. *Plant Physiol* 125:935–942.
8. Bergmann DC, Sack FD (2007) Stomatal development. *Annu Rev Plant Biol* 58:163–181.
9. Berner RA (2006) Inclusion of the weathering of volcanic rocks in the GEOCARBSULF model. *Am J Sci* 306:295–302.
10. van de Water PK, Leavitt SW, Betancourt JL (1994) Trends in stomatal density and $^{13}C/^{12}C$ ratios of *Pinus flexilis* needles during last glacial-interglacial cycle. *Science* 264:239–243.
11. Beerling DJ, Chaloner WG, Huntley B, Pearson JA, Tooley MJ (1993) Stomatal density responds to the glacial cycle of environmental-change. *Proc R Soc London Ser B* 251:133–138.
12. Woodward FI (1987) Stomatal numbers are sensitive to increases in CO_2 from preindustrial levels. *Nature* 327:617–618.
13. Long SP, Ainsworth EA, Rogers A, Ort DR (2004) Rising atmospheric carbon dioxide: plants FACE the future. *Annu Rev Plant Biol* 55:591–628.
14. Fletcher BJ, Brentnall SJ, Anderson CW, Berner RA, Beerling DJ (2008) Atmospheric carbon dioxide linked with Mesozoic and early Cenozoic climate change. *Nat Geosci* 1:43–48.
15. Salisbury EJ (1928) On the causes and ecological significance of stomatal frequency, with special reference to the woodland flora. *Philos Trans R Soc London Ser B* 216:1–65.
16. Gindel I (1969) Stomatal number and size as related to soil moisture in tree xerophytes in Israel. *Ecology* 50:263–267.
17. Clifford SC, et al. (1995) The effect of elevated atmospheric CO_2 and drought on stomatal frequency in groundnut (*Arachis hypogaea* L.). *J Exp Bot* 46:847–852.
18. Driscoll SP, Prins A, Olmos E, Kunert KJ, Foyer CH (2006) Specification of adaxial and abaxial stomata, epidermal structure and photosynthesis to CO_2 enrichment in maize leaves. *J Exp Bot* 57:381–390.
19. Assmann SM, Zeiger E (1987) Guard cell bioenergetics. *Stomatal Function*. eds Zeiger E, Farquhar GD, Cowan IR (Stanford Univ Press, Palo Alto, CA), pp 163–193.
20. Srivastava A, Lu Z, Zeiger E (1995) Modification of guard cell properties in advanced lines of Pima cotton bred for higher yields and heat resistance. *Plant Sci* 108:125–131.
21. Woodward FI, Kelly CK (1995) The influence of CO_2 concentration on stomatal density. *New Phytol* 131:311–327.
22. Royer DL (2001) Stomatal density and stomatal index as indicators of paleoatmospheric CO_2 concentration. *Rev Palaeobot Palynol* 114:1–28.
23. Lake JA, Woodward FI (2008) Response of stomatal numbers to CO_2 and humidity: control by transpiration rate and stomatal numbers. *New Phytol* 179:397–404.
24. Bergmann DC, Lukowitz W, Somerville CR (2004) Stomatal development and pattern controlled by a MAPKK kinase. *Science* 304:1494–1497.
25. Franks PJ, Beerling DJ (2009) CO_2-forced evolution of plant gas exchange capacity and water-use efficiency over the Phanerozoic. *Geobiology* 7:227–236.
26. Niklas KJ, Tiffney BH, Knoll AH (1983) Patterns in vascular land plant diversification. *Nature* 303:614–616.
27. Sperry JS (2003) Evolution of water transport and xylem structure. *Int J Plant Sci* 164:S115–S127.
28. Cowan IR, Farquhar GD (1977) Stomatal function in relation to leaf metabolism and environment. *Integration of Activity in the Higher Plant*. ed Jennings DH (Cambridge Univ Press, Cambridge, UK), pp 471–505.
29. Franks PJ, Farquhar GD (1999) A relationship between humidity response, growth form and photosynthetic operating point in C_3 plants. *Plant Cell Environ* 22:1337–1349.
30. Beerling DJ, Berner RA (2005) Feedbacks and the coevolution of plants and atmospheric CO_2. *Proc Natl Acad Sci USA* 102:1302–1305.
31. Uprety DC, Dwivedi N, Jain V, Mohan R (2002) Effect of elevated carbon dioxide concentration on the stomatal parameters of rice cultivars. *Photosynthetica* 40:315–319.
32. Vanhatalo R, Huttunen S, Back J (2001) Effects of elevated [CO2] and O3 on stomatal and surface wax characteristics in leaves of pubescent birch growth under field conditions. *Trees–Structures and Function* 15:304–313.